

## A Computational Approach to the Structure of 4-Alkoxy-4'-cyanobiphenyl in Nematic Mesophase

Isamu ONO and Shoichi KONDO\*

Department of Chemistry, Faculty of Science, Science University of Tokyo, 1-3 Kagurazaka, Shinjuku-ku, Tokyo 162  
(Received August 11, 1992)

Computer simulations were carried out to study the structural properties of the nematogens, *n*OCB (*n*=5–8). The order parameters for the individual C–H bonds in the alkoxy chain decreased stepwise along the chain in a manner similar to that determined by NMR techniques. A small difference in the ratio of molecular length to width for the compounds studied appeared according to the flexibility in the chain. The calculated densities and anisotropies in the self-diffusion coefficients were found to decrease with increasing number of carbons in the chain.

Molecular dynamics (MD) or Monte Carlo (MC) simulations using particles such as the hard-body model are now employed as an approach to the phase transitions of liquid crystals.<sup>1)</sup> It was established to a certain extent that an anisotropy of molecular shape, e.g., the ratio of molecular length to width, is required for the appearance of the liquid crystal phase, and the simulation results coincided basically with the theoretical results. However, it is difficult to evaluate the anisotropy of molecular shape for actual compound with intricate structures in mesophase.

4-Alkoxy-4'-cyanobiphenyl (*n*OCB), which is a typical liquid crystalline compound with a rod-like shape, has a cyanobiphenyl part and an alkoxy chain, in which *n* denotes the number of carbons in the alkoxy chain. Liquid crystalline characters are dependent on the length of the chain. Enantiotropic nematic phases are exhibited for *n*OCB from *n*=5 to 9. In the nematic phase, the order parameters of each bond decrease along the alkoxy chain, because the chains have a flexible structure.<sup>2)</sup> The structural properties in the nematic phase should be evaluated by considering the conformation or flexibility of the side chain.

MD simulation based on an atom–atom potential for actual molecules is expected to evaluate the molecular structure in the mesophase. But the simulation is fairly restricted, because the computation takes a very long time. A few studies were reported about molecular ordering in the nematic phase by MD simulation for a system of 64–128 molecules.<sup>3,4)</sup> In our preliminary calculation using a canonical ensemble for 5OCB, the MD simulation is able to obtain the ordering not only of a whole molecule but also of the side chain attributed to its flexibility.<sup>5)</sup> Moreover, we recently reported the ordering of the side chain of a disk-like molecule of hexakis(pentyloxy)triphenylene (THE5) in the discotic mesophase.<sup>6)</sup>

We performed MD simulations using the isobaric and isothermal ensemble for *n*OCB (*n*=5, 6, 7, and 8) assumed to be in the nematic phase. The calculated order parameters were compared with the experimental results from <sup>13</sup>C NMR.<sup>2)</sup> We also evaluated the conformation and the anisotropy of the molecular shape in the

nematic phase.

### Computation

The potential energy used in the MD simulation<sup>5,6)</sup> is

$$E = E_{\text{ES}} + E_{\text{VDW}} + E_{\text{TORS}}.$$

The Coulomb potential  $E_{\text{ES}}$  is

$$E_{\text{ES}} = Q_i Q_j / r_{ij},$$

where  $Q_i$  and  $Q_j$  are the atomic charges of atoms *i* and *j*, respectively, and  $r_{ij}$  is the distance between atoms *i* and *j*. The atomic charges were calculated using the ab initio molecular orbital method (STO-3G) for an isolated molecule. For the van der Waals term ( $E_{\text{VDW}}$ ), the potential function used in molecular mechanics MM2<sup>7)</sup> was adopted,

$$E_{\text{VDW}} = 2.90 \times 10^5 \varepsilon \exp(-12.50 r_{ij}/r_0) - 2.25 \varepsilon (r_0/r_{ij})^6,$$

$$\varepsilon = \sqrt{\varepsilon_i \varepsilon_j} \quad \text{and} \quad r_0 = r_i + r_j,$$

where  $\varepsilon_i$  and  $r_i$  are the constants for atom *i*. The values adopted in this calculation are as follows; 0.23 kJ mol<sup>-1</sup> and 0.182 nm for nitrogen, 0.18 kJ mol<sup>-1</sup> and 0.194 nm for carbon, and 0.20 kJ mol<sup>-1</sup> and 0.182 nm for hydrogen, respectively.<sup>7)</sup> The methylene groups in the aliphatic chain were approximated as being united atoms ( $\varepsilon_i=0.17$  kJ mol<sup>-1</sup> and  $r_i=0.200$  nm).<sup>5)</sup> The torsion term ( $E_{\text{TORS}}$ ) for the alkoxy chain was calculated as follows,

$$E_{\text{TORS}} = V_1(1 + \cos \omega) + V_3(1 + \cos 3\omega).$$

The parameters,  $V_1=2.51$  kJ mol<sup>-1</sup> and  $V_3=4.81$  kJ mol<sup>-1</sup> for the O–C bond and  $V_1=2.51$  kJ mol<sup>-1</sup> and  $V_3=4.18$  kJ mol<sup>-1</sup> for other bonds, were selected by considering the results of the mean field approximation for *n*OCB.<sup>8)</sup> A value of 0.8 nm<sup>4)</sup> was adopted as the cut-off radius in the MD. In the MD simulation, all the lengths and angles of the bonds were fixed to the standard values defined by MM2.<sup>7)</sup> For the angles of C<sub>ar</sub>–O–C<sub>1</sub> and O–C<sub>1</sub>–C<sub>2</sub>, which were important to determine the order parameter of the alkoxy chain, the

values used in Ref. 8, i.e.,  $116^\circ$  and  $120^\circ$ , were adopted, respectively.

An isobaric and isothermal ( $NTP$ ) ensemble<sup>9,10</sup> under atmospheric pressure was used for the MD simulation. A periodic boundary condition was adopted for the rectangular unit cell.<sup>4</sup> The equations of motion were integrated using a leapfrog scheme.<sup>11</sup> The MD run took sixty thousand time steps of three femtoseconds each; during the initial six thousand steps, the calculation was carried out at a higher temperature so as to avoid any dependence on the initial geometry.

All calculations were performed on a HITAC M-880/310 located in the Computer Center of the University of Tokyo.

## Results and Discussion

**Structure of the Isolated Molecule.** The structure was optimized by standard molecular mechanics MM2<sup>7</sup>) for the isolated  $n$ OCB molecules. All-*trans* structures were obtained for the most stable conformation. It is predicted that these extended structures preferentially exist in the mesophase, because their molecular structures are linear shapes. To estimate an anisotropy of the molecular shape, we calculated the ratio of the molecular length ( $l$ ) to the molecular width ( $d$ ). The value of  $l$  was defined as the maximum length along the principal axis of inertia for the molecule. The value of  $d$  was defined as the diameter of the minimum cylinder which contains the whole molecule. The ratio  $l/d$  depends on the conformation of the alkoxy chain of  $n$ OCB. For example, the ratios of the all-*trans* conformer and five conformations with a *gauche* for 6OCB are shown in Fig. 1. But the values of  $l/d$  in the nematic phase should be estimated from the population of the conformations which exist in the nematic phase.

**Calculation of the Dimer.** In order to clarify the intermolecular configuration of the dimer, we next performed the energy calculation using the same potential as in the MD simulation. Figure 2 shows the contour map of intermolecular energy as a function of the intermolecular distance ( $r$ ) and rotational angle ( $\theta$ ). The conformation of the side chain is assumed to be all *trans*, and the dihedral angle of the two phenyl ring is fixed to  $30^\circ$ . The two molecules are separated by a distance of about 0.35 nm with rotational angles of  $200^\circ$  or  $20^\circ$  in the stable configurations, and the anti parallel arrangement ( $200^\circ$ ) is slightly more stable than the parallel arrangement ( $20^\circ$ ). This is consistent with the conventional results of calculations for compounds with cyanobiphenyl.<sup>12</sup>)

**MD Simulation in the Nematic Phase.** In liquid crystal phases, molecules are condensed and aligned. We restricted the number of molecules to 64 due to the very long computational time. The initial geometries were estimated from the results of X-ray diffraction<sup>13</sup>) for the crystal, and the initial MD runs were performed at higher temperatures to avoid any dependence on the

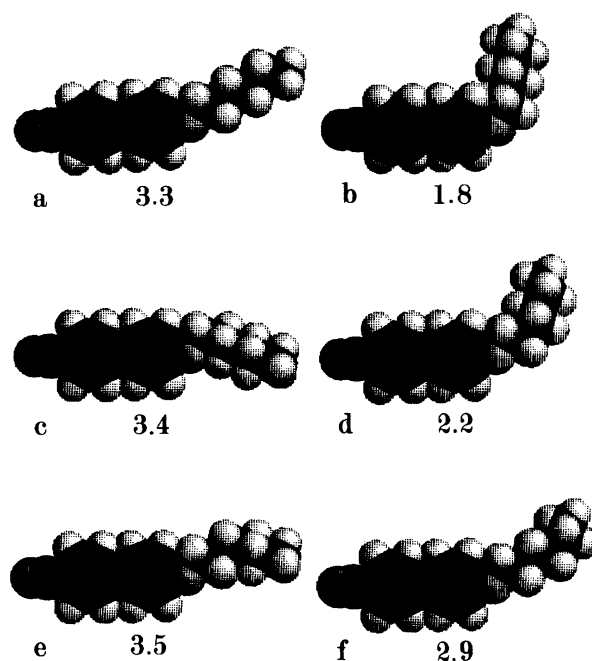


Fig. 1. Six conformers of 6OCB and their  $l/d$  values. Conformations are as follows, a: *ttttt*, b: *gtttt*, c: *tggtt*, d: *ttgtt*, e: *tttgt*, and f: *ttttg*.

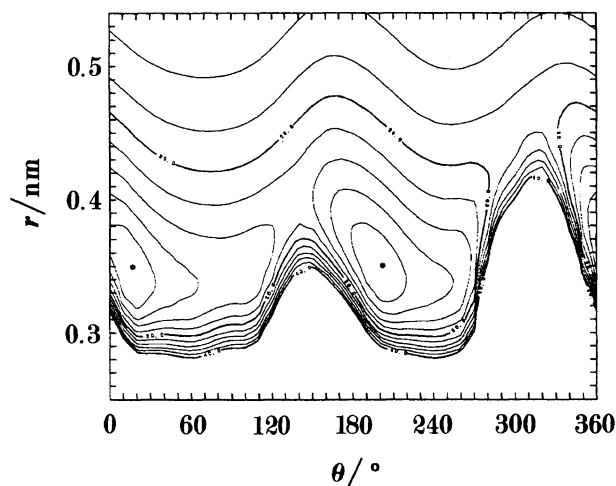


Fig. 2. Contour map of relative energy for a pair of 6OCB molecules which are arranged with the intermolecular distance ( $r$ ) and the angle of molecular axes ( $\theta$ ).

starting geometry.

We first performed the MD simulation for 6OCB at 330, 339, and 359 K, in which the temperatures, 330 and 339 K, correspond experimentally to those in the nematic phase. Figure 3 shows a *snapshot* taken at 339 K, and Table 1 lists the simulated results after equilibrium was reached. The order parameters  $P_2$  and  $P_4$ , which were defined by the axis of the biphenyl, decreased according to the increment of temperature. The values of  $P_2=0.55$  at 330 K and  $P_2=0.50$  at 339 K seem reasonable for the order parameter in the nematic

Table 1. Calculated Density, Order Parameters and Self-Diffusion Coefficients for 6OCB at 330, 339, and 359 K

$\frac{T}{K}$	$\frac{\rho}{10^{-3} \text{ kg m}^{-3}}$	$P_2$	$P_4$	$\frac{D_{\parallel}}{10^{-10} \text{ m}^2 \text{ s}^{-1}}$	$\frac{D_{\perp}}{10^{-10} \text{ m}^2 \text{ s}^{-1}}$	$D_{\parallel}/D_{\perp}$
330	0.95	0.55	0.15	2.80	1.13	2.47
339	0.94	0.50	0.10	3.30	1.68	1.96
359	0.91	0.28	-0.05	3.05	2.40	1.27

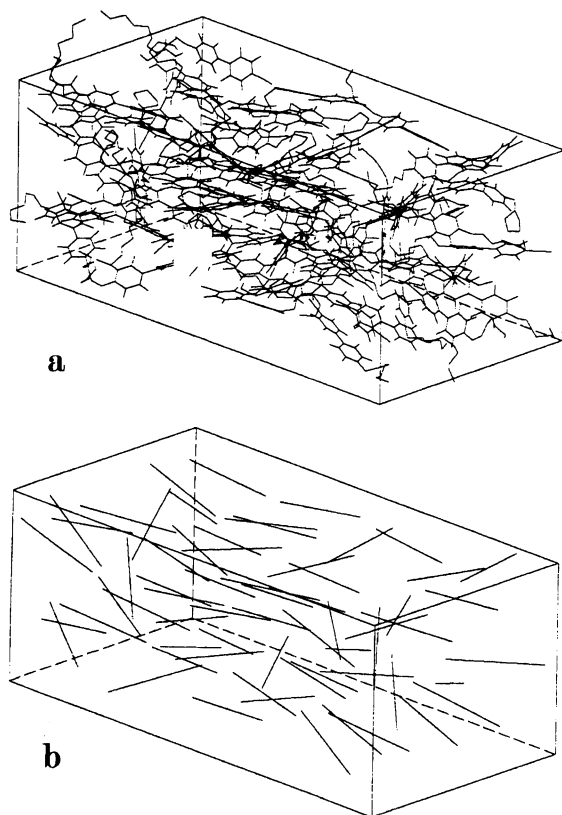


Fig. 3. Snapshots of 64 molecules of 6OCB at 339 K. a: Whole molecules, b: molecular axes.

phase. An anisotropy of the self-diffusion coefficient,  $D$ , is usually observed in an anisotropic system such as the liquid crystal. Especially, the self-diffusion coefficient along the director,  $D_{\parallel}$ , is greater than that perpendicular to the director,  $D_{\perp}$ , in the nematic phase.<sup>14)</sup> We calculated  $D$  from the slope of the mean square displacement (MSD) in the MD simulation. Figure 4 shows the result for 6OCB at 339 K, which is averaged at intervals of five thousand steps for the final thirty thousand steps. The anisotropy in the self-diffusion coefficients ( $D_{\parallel}/D_{\perp}$ ) calculated from the MSD was clearly shown (see Table 1). As judged by the results of the order parameter and the self-diffusion coefficient, the molecular ordering and motion in the nematic phase were reproduced by the MD simulation. The temperature 359 K experimentally corresponds to that in the isotropic phase. The order parameters and the anisotropy of  $D$  were small compared with those in the nematic phase.

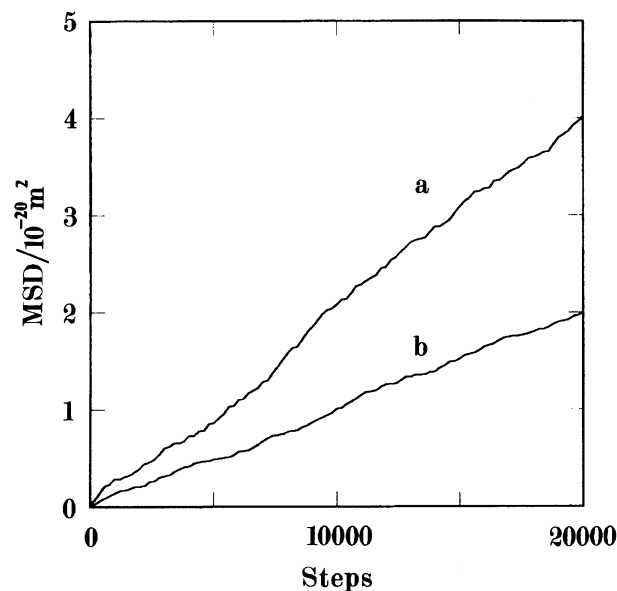


Fig. 4. Plots of MSD for parallel (a) and perpendicular (b) components to the director of 6OCB at 339 K.

Although the value of  $P_2$  is not equal to 0, these results are similar to those from our preliminary simulation<sup>5)</sup> and others.<sup>3,4)</sup>

We next calculate the MD for *n*OCB in the nematic phase in order to discuss the dependency of the physical properties on the length of the alkoxy chain. Simulated temperatures 331 K (5OCB), 339 K (6OCB), 337 K (7OCB), and 342 K (8OCB) correspond to the  $T_{\text{NI}} - 10$  K, where  $T_{\text{NI}}$  is the experimental transition temperature between the nematic and isotropic phases. We selected these temperatures to compare with the experimental results. Table 2 shows the calculated density, order parameters, and self-diffusion coefficients. It appears that the density decreases with increasing chain length. These values agreed with the experimental density observed by one of the authors within errors of about 10%.<sup>15)</sup> On the order parameters, calculated  $P_2$  were about 0.5, corresponding to the experimental values in the nematic phase.<sup>2)</sup> A clear consensus on the magnitude of  $P_4$  has not been given by experiments, the values obtained are of the order 0.1 as shown in Table 2. The anisotropy of  $D$  was also obtained for each *n*OCB. As described previously, the molecular ordering and motion for *n*OCB in the nematic phase were reproduced by MD simulation. It was perceived that  $P_2$ ,  $P_4$  and  $D_{\parallel}/D_{\perp}$  decreased with increasing carbon number

Table 2. Calculated Density, Order Parameters and Self-Diffusion Coefficients for *n*OCB

<i>n</i>	$\frac{T}{K}$	$\frac{\rho}{10^{-3} \text{ kg m}^{-3}}$	$P_2$	$P_4$	$\frac{D_{\parallel}}{10^{-10} \text{ m}^2 \text{ s}^{-1}}$	$\frac{D_{\perp}}{10^{-10} \text{ m}^2 \text{ s}^{-1}}$	$D_{\parallel}/D_{\perp}$
5	331	0.98	0.53	0.12	3.60	1.88	1.91
6	339	0.94	0.50	0.10	3.30	1.68	1.96
7	337	0.94	0.50	0.11	3.16	1.76	1.80
8	342	0.90	0.47	0.08	2.82	1.77	1.59

in the alkoxy chain. But a clear odd-even effect was not seen in  $P_2$ ,  $P_4$  and  $D_{\parallel}/D_{\perp}$ .

We will now discuss the molecular conformation owing to the flexibility of the side chain in the nematic phase. In the simulation, the rates of conformational change among the *trans* and two *gauche* were observed, e.g.,  $1.6 \times 10^{10} \text{ s}^{-1}$  and  $6.5 \times 10^{10} \text{ s}^{-1}$  for the O-C<sub>1</sub> and C<sub>4</sub>-C<sub>5</sub> bonds in 6OCB at 339 K, respectively. For each *n*OCB, the rate in the terminal bond was larger than that in the inner bond. By analyzing the NMR relaxation behavior, the *g*→*t* transition rates in 5CB were  $3.0 \times 10^9 \text{ s}^{-1}$  for the inner bond and  $1.6 \times 10^{10} \text{ s}^{-1}$  for the terminal bond.<sup>16)</sup> On the other hand, the order parameters of each C-H bond ( $P_2(\text{CH})$ ) in the alkoxy chain were observed in the nematic phase by <sup>13</sup>C NMR studies.<sup>2)</sup> The values of  $P_2(\text{CH})$  can be calculated from the conformation of the alkoxy chain,<sup>5)</sup> even though the methylene groups are treated as being united atoms in the MD simulation. Figure 5 shows the calculated  $P_2(\text{CH})$  (closed circle) against the bond position. The value of  $P_2(\text{CH})$  decreases stepwise along the alkoxy chain. Such a decrease in  $P_2$  is in agreement with that of the experimental values (open circles),<sup>2)</sup> while the quantitative agreement is inferior to the results of a

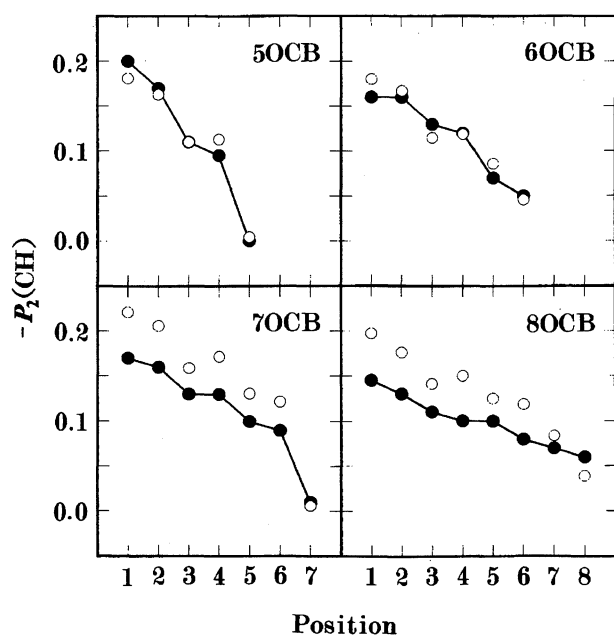


Fig. 5. Calculated (●) and experimental<sup>2)</sup> (○) order parameters ( $P_2(\text{CH})$ ) against the bond position.

mean field approximation<sup>8,17)</sup> or of our preliminary simulation using a canonical ensemble.<sup>5,6)</sup> To discuss the conformation of the alkoxy chain, the probability of a *trans* conformer, which has values from 120° to 240° as the dihedral angle, against the bond position is shown in Fig. 6. The closed circles and open squares correspond to the results of the MD assumed in the nematic phase and of the MC simulation for the isolated *n*OCB at the temperatures, respectively. Comparing with the results of the isolated *n*OCB, the population of a *trans* conformer in the nematic phase is dependent on the bond position. The relatively large populations for the odd positions in an alkoxy chain are instructive. This tendency is usually observed in liquid crystals, and is assigned to the effect of the anisotropy in the molecular shape as a result of the excluded volume effect. *Trans* conformations in the odd positions have a large influence on the linearity of the molecules.

To evaluate the anisotropy of the molecular shape, the ratio  $l/d$  was also calculated in a manner similar

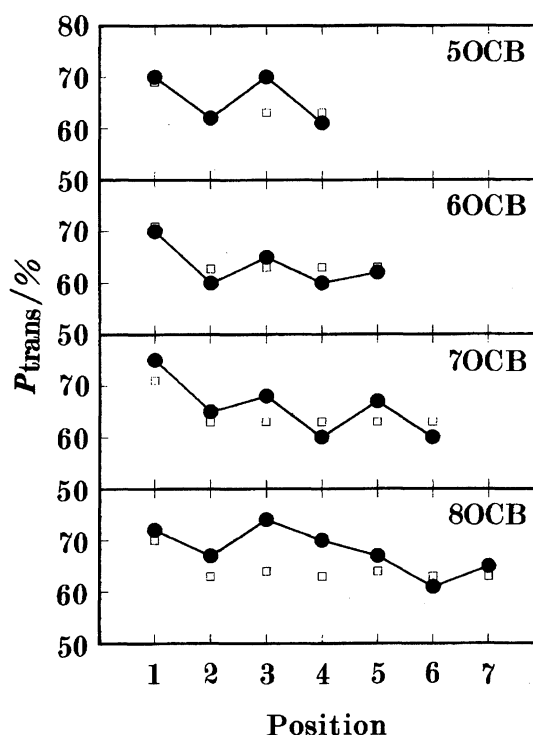


Fig. 6. Population of the *trans* conformer for each bond in the alkoxy chain of *n*OCB. ●: Nematic, □ Isolated.

to that given for the structure of the isolated molecule. Figure 7 shows the population of  $l$  and  $d$  for 6OCB in the nematic phase (solid lines) and in the isolate (dashed lines) at 339 K. In each case,  $d$  distributes from 0.4 to 1.0 nm, and  $l$  distributes from 1.0 to 1.8 nm. It can be seen that the distribution curves become narrower, and the populations at around 0.5 nm in  $d$  and at around 1.8 nm in  $l$  become large as the system goes from the isolated to the nematic phase. It indicates the increase of an anisotropy in the molecular shape due to the molecular ordering in the nematic phase. Figure 8 shows the population of  $l/d$  for *n*OCB. Solid and dashed lined also

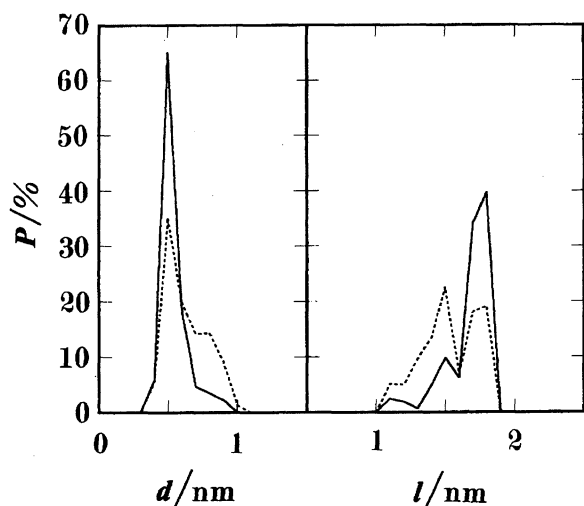


Fig. 7. Distributions of  $d$  and  $l$  of 6OCB at 339 K. —: Nematic, ---: Isolated.

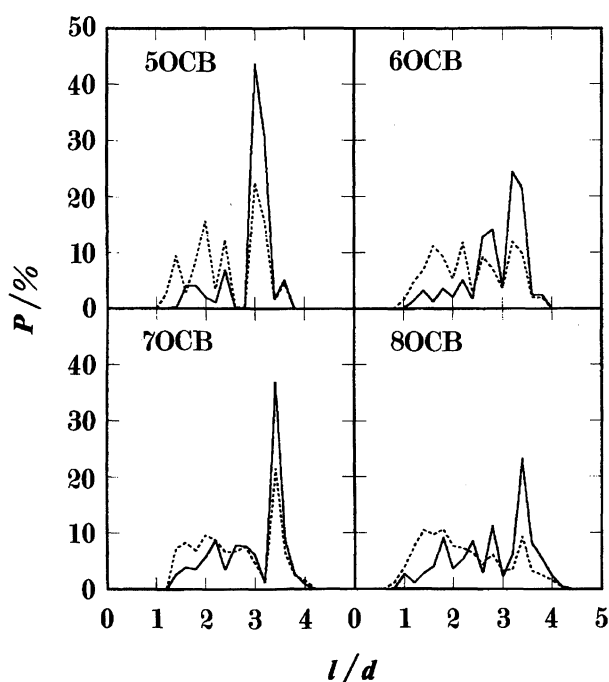


Fig. 8. Distributions of the ratio  $l/d$  of *n*OCB. —: Nematic, ---: Isolated.

correspond to the result in the nematic phase and in the isolate, respectively. The anisotropy indicated by  $l/d$  is clearly larger in the nematic phase than in the isolate. In the nematic phase, the ratios with the most probability were 3.0 (5OCB), 3.2 (6OCB), 3.4 (7OCB) and 3.4 (8OCB), but the averaged values were calculated to be about 2.9 for each *n*OCB.

In this MD simulation using realistic molecules, the molecular ordering and motion in the nematic phase were reproduced for four compounds from 5OCB to 8OCB. Moreover, it is clear that the flexibility of the side chain is an important factor governing the structural properties of liquid crystals. Although the validity of the simulating conditions should be further considered from calculations in various conditions such as computing method, geometry and potential parameter etc., the results in this work show that MD simulations using realistic molecules may allow the study of molecular structures in the nematic mesophase.

The authors thank Professor Masatami Takeda at the Science University of Tokyo for his helpful discussions.

## References

- 1) For example: J. Vieillard, *J. Chem. Phys.*, **56**, 4729 (1972); A. Stroobants, H. N. W. Lekkerkerker, and D. Frenkel, *Phys. Rev. A*, **36**, 2929 (1987); J. G. Gay and B. J. Berne, *J. Chem. Phys.*, **74**, 3316 (1981).
- 2) C.-D. Poon, C. M. Wooldridge, and B. M. Fung, *Mol. Cryst. Liq. Cryst.*, **157**, 303 (1988).
- 3) S. J. Picken, W. F. Van Gunsteren, P. TH. Van Duijnen, and W. H. De Jeu, *Liq. Cryst.*, **6**, 357 (1989).
- 4) M. R. Wilson and M. P. Allen, *Mol. Cryst. Liq. Cryst.*, **198**, 465 (1991); *Liq. Cryst.*, **12**, 157 (1992).
- 5) I. Ono and S. Kondo, *Mol. Cryst. Liq. Cryst. Lett.*, **8**, 69 (1991).
- 6) I. Ono and S. Kondo, *Bull. Chem. Soc. Jpn.*, **65**, 1057 (1992).
- 7) N. L. Allinger, *J. Am. Chem. Soc.*, **99**, 8127 (1977); C. Jaime and E. Osawa, *Tetrahedron*, **39**, 2769 (1983), and references therein.
- 8) C. J. R. Counsell, J. W. Emsley, G. R. Luckhurst, and H. S. Sachdev, *Mol. Phys.*, **63**, 33 (1988).
- 9) S. Nosé, *Mol. Phys.*, **52**, 255 (1984); *J. Chem. Phys.*, **81**, 511 (1984).
- 10) H. C. Andersen, *J. Chem. Phys.*, **72**, 2384 (1980).
- 11) R. W. Hockney, *Methods Comput. Phys.*, **9**, 135 (1970).
- 12) M. R. Wilson and D. A. Dunmur, *Liq. Cryst.*, **5**, 987 (1989).
- 13) P. Mandal and S. Paul, *Mol. Cryst. Liq. Cryst.*, **131**, 223 (1985).
- 14) G. J. Krüger, *Phys. Report*, **82**, 229 (1982), and references therein.
- 15) M. Aoshima, S. Mita, and S. Kondo, "61st National Meeting of the Chemical Society of Japan," March 1991, Abstr., No. 3E314.
- 16) A. Ferrarini, L. Nordio, and G. J. Moro, *Mol. Cryst. Liq. Cryst.*, **198**, 159 (1991).

- 17) D. J. Photinos, E. T. Samulski, and H. Toriumi, *J. Chem. Phys.*, **94**, 2758 (1991).
-